Mechanical Systems and Signal Processing 24 (2010) 2235–2249

Contents lists available at ScienceDirect

Mechanical Systems and Signal Processing

journal homepage: www.elsevier.com/locate/jnlabr/ymssp

Torsion and transverse sensing of conical shells

H. Li [a,*], Z.B. Chen [a], H.S. Tzou [b]

[a] School of Mechatronics Engineering, Harbin Institute of Technology, Harbin, China
[b] Structronics Laboratory, Department of Mechanical Engineering, University of Kentucky, Lexington, KY 40506-0503, USA

ARTICLE INFO

Article history:
Received 24 March 2010
Received in revised form
7 May 2010
Accepted 9 May 2010
Available online 26 May 2010

Keywords:
Conical shell
Vibration
Distributed sensing
Shear-type sensor
Diagonal piezoelectric patch

ABSTRACT

Conical shells are widely used as payload/rocket adapters in rocket fairing systems. Generally, the conical shells are clamped at the major end and free at the minor end, where the payload is mounted. This study focuses on the dynamic sensing of conical shells with fix-free boundary conditions (BCs) by using distributed piezoelectric helical sensors. Two types of motion are studied, i.e., the transverse modes and the torsion modes. The shear-type sensors for shells sensing are presented first. Formulations of sensing signals of a general shell of revolution are presented, and then simplified to conical shells. For sensing of transverse vibrations, thin piezoelectric sensors are laminated on the top surface. Two types of sensor distribution are considered: a fully distributed and a helical or diagonal laminated. The total signal consists of four components resulting from the four strain components, and each of them is evaluated in detail. For sensing of torsion vibrations, a meridional polarized shear-type sensor with side electrodes is layered on the top surface of the shell structure. Sensing signals of natural shell modes are also evaluated. Analyses show that, in low order modes, the sensing signals induced by the circumferential membrane strains are the primary components of the total signal generations. The numerical results indicate the optimal location of the sensors. The proposed method is capable of determining the modal participation factors, while the testing signal is available; it is also capable of determining the mode shapes by using several distributed sensor segments.

1. Introduction

Conical shells are widely used structures, such as whole-spacecraft adapters, supporters. In some precise applications, severe vibration propagates to the supported payload through the conical shell, which may cause precision loss or damage [1,2]. Precise measurements of the vibration are necessary for shape control and active isolation of the structures, and the distributed piezoelectric sensor gets most attention because of their light weight, less energy conversion and less power consumption [3,4].

The signals of distributed piezoelectric sensors are functions of the inner strain, and can be used to represent the characteristics of structure deformation or fracture [5,6]. So the piezoelectric sensor is applicable of vibration sensing, healthy monitoring and so on. Wu et al. [7] investigated the electromechanical behavior of piezoelectric generic shells using a high order theory. Callahan and Baruh [8] utilized rectangular sensor to detect the vibration of circular cylindrical

* Corresponding author. Tel: +86 451 86412057.
E-mail address: Lhlihua@gmail.com (H. Li).

0888-3270/$ - see front matter © 2010 Elsevier Ltd. All rights reserved.
doi:10.1016/j.ymssp.2010.05.004

shells. Chai and Tzou [9] investigated the distributed sensing characteristics of conical shell, and proved that the sensing signals of each mode consisted of four components, related to the four strain items, i.e., longitudinal membrane strain, circumferential membrane strain, longitudinal bending strain and circumferential bending strain. It was assumed that the piezoelectric sensors were not sensitive to in-plane shear deformation. As a result, the proposed sensor is not applicable for the sensing of torsional vibrations.

The shear-type piezoelectric devices were proposed by Sun and Zhang in 1990s [10]. They presented a preliminary static evaluation of the concept of piezoelectric shear actuation on a cantilever sandwich beam structure. Glazounov et al. [11] proposed a piezoelectric actuator generating angular displacement using the shear piezoelectric effect. Benjeddou and Deu [12] investigated the transverse shear actuation and sensing of plates using an exact three-dimensional mixed state space formulation. Baillargeon et al. [13] presented the experimental and numerical assessment of the active vibration suppression of smart structures using piezoelectric shear actuators.

In practical applications, the major end of the conical adapter is fixed to the launch vehicle and the minor end is connected to the payload. The payload is excited to vibrate in axial, lateral and torsional directions [14,15]. Therefore, the distributed sensing of the vibrations of conical shell with clamped-free BCs still needs to be further developed.

This paper focuses on the sensing signals of the truncated conical shells, including transverse vibration and torsions. The BCs are assumed to be clamped at the major end and free at the minor end. The sensing signals are investigated based on the thin shell assumption.

For shells in torsion vibration, general sensing equation is proposed and adapted to conical shell with fixed-free BCs. The distributed modal voltage is derived, and the first two modes are demonstrated. The shear deformation can be analytically solved using the proposed equation; the signal can be used as a feedback or control signal during the active vibration suspension. For sensing of transverse vibrations, two types of sensor layer distributions are considered: full and diagonal sensing. The displacement functions for fixed-free conical shells are presented, followed by the derivation of sensing equations. Then the distributed sensing signal and its components are studied in detail. The results prove that the distributed sensing signals are identical with the distribution of the strain. And the optimal locations of piezoelectric sensors can be defined accordingly.

2. Design of shell torsion sensors

Since the objective of this study is to evaluate torsional and transverse sensing behavior of conical shells, the electric field generation of piezoelectric materials due to shear strains is discussed first in this session. The signal induced by a generic shell sensor patch laminated on an elastic shell with shear deformations is defined next and followed by its application to torsion sensing of conical shells.

2.1. Shear-type sensors

Fig. 1a shows a general piezoelectric cubic, in which the arrow P denotes the polarized direction. For the piezoelectric cubic shown in Fig. 1a, two types of cutting pieces can be utilized to work in the shear mode, as illustrated in Fig. 1b and c [16]. According to the converse piezoelectric effect, the piezoelectric materials induce a shear deformation when the driving voltage is applied perpendicular to the poling direction.

On the other hand, based on the direct piezoelectric effect, an electric field is established between the electrodes when the piezoelectric patch is subjected to shear deformations. The resultant voltage between the electrodes can be measured. The electric field of the piezoceramic can be described as [17]

$$\boldsymbol{E} = \boldsymbol{\beta}^{S}\boldsymbol{D} - h\boldsymbol{S} \tag{1}$$

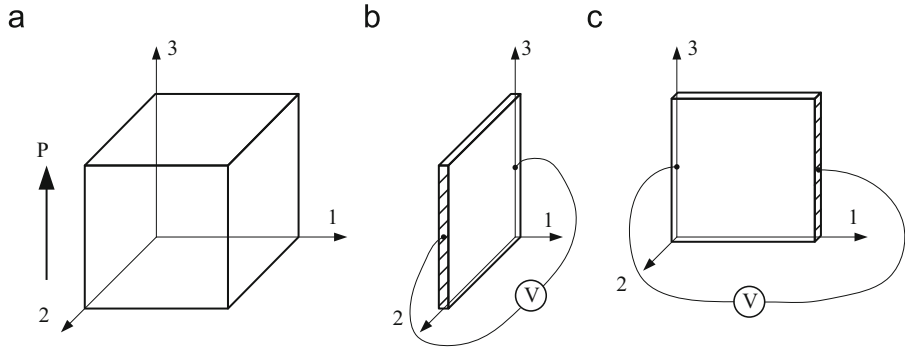

Fig. 1. Two shear modes of piezoceramic.

where $\boldsymbol{E}$ is the electric field vector; $\boldsymbol{D}$ is the electric displacement vector; $\boldsymbol{S}$ is the strain vector; $\boldsymbol{\beta}^S$ and $\boldsymbol{h}$ are matrices defined as

$$\boldsymbol{\beta}^S = \begin{bmatrix} \beta_{11}^S & & \\ & \beta_{11}^S & \\ & & \beta_{33}^S \end{bmatrix} \tag{2}$$

$$\boldsymbol{h} = \begin{bmatrix} & & & h_{15} & 0 \\ & & h_{15} & & 0 \\ h_{31} & h_{31} & h_{33} & & 0 \end{bmatrix} \tag{3}$$

For piezoelectric patch works in shear mode, as shown in Fig. 1b, the inner electric field related to the in-plane shear deformation S_{23} is given by

$$E_2 = \beta_{11}^S D_2 - h_{15} S_4 \tag{4}$$

On the other hand, for a piezoelectric patch shown in Fig. 1c, the electric field is given by

$$E_1 = \beta_{11}^S D_1 - h_{15} S_5 \tag{5}$$

2.2. Torsional sensing voltage for shells

The shell-type sensor is cut piecewise from a piezoceramic shell polarized in the longitudinal direction, and it works in shear mode, as shown in Fig. 2.

For thin conical shell in torsional vibrations, the strain components S_1, S_2, S_4, S_6 are zeros. Assuming that the electric charge is balanced in the piezoelectric sensor layer, one can derive the electrical charge equation by using the Gauss theorem [5].

$$\nabla\{D_i\} = 0 \tag{6}$$

where ∇ is a differential operator. According to the Maxwell's equation, the electric field E_i can be related to the electric potential ϕ by

$$\{E_i\} = \nabla\phi \tag{7}$$

The voltage across the electrodes can be obtained by integrating the electric field along the electric field direction, i.e.,

$$\phi = -\int E_1 A_2 \, d\alpha_2 \tag{8}$$

when the piezoelectric sensor layer is subjected to shear deformation, the inner electric field between the electrodes can be expressed in Eq. (5). Rearranging the equation yields

$$D_1 = \frac{1}{\beta_{11}^S}(E_1 + h_{15} S_5) \tag{9}$$

Since D_1 is defined as the charge per unit area [5], one can integrate the former equation over the electrode surface S^e to estimate a total surface charge.

$$\int_{S^e} D_1 \, dS^e = \int_{S^e} \frac{1}{\beta_{11}^S}(E_1 + h_{15} S_5) \, dS^e \tag{10}$$

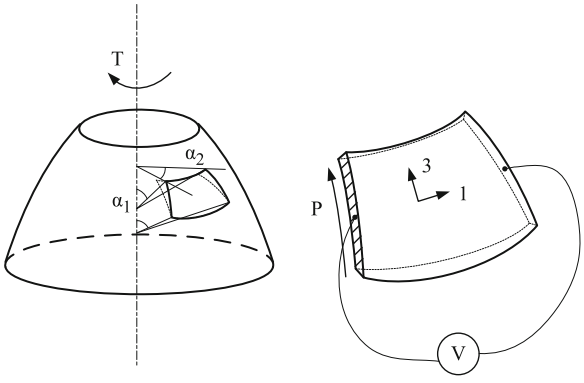

Fig. 2. A piezoelectric shell of revolution. The arrow P indicates the polarized direction.

In general, the dielectric constants of piezoelectric materials are much larger than those of the free space, D_1 can be set as zero [18]

$$\int_{S^e} \frac{1}{\beta_{11}^S}(E_1 + h_{15}S_5)\,dS^e = 0 \tag{11}$$

The electric field is estimated as

$$E_1 = -\frac{1}{S^e}\int_{S^e} h_{15}S_5\,dS^e \tag{12}$$

where S^e is the electrode area. It is assumed that the piezoelectric sensor has uniform thickness h^S. Its electrode area can be expressed as

$$S^e = h^S \int A_1\,d\alpha_1 \tag{13}$$

where A_1 is the Lamé parameter. The voltage across the electrodes can be obtained by integrating the electric field over the length of the piezoelectric sensor layer, i.e.,

$$\phi^s = -\int_{\alpha_2} E_1 A_2\,d\alpha_2 \tag{14}$$

where A_2 is the Lamé parameter. Substituting the electric field yields the voltage signal with respect to shear strain S_5

$$\phi^s = \frac{h_{15}}{S^e}\int_{\alpha_2}\int_{S^e} S_5 A_2\,dS^e\,d\alpha_2 = \frac{h_{15}}{S^e}\int_{\alpha_1}\int_{\alpha_2}\int_{z} S_5 A_1 A_2\,d\alpha_1\,d\alpha_2\,dz \tag{15}$$

Eq. (15) is the signal generation for a generic shell of revolution, applicable to sense any type of shells of revolution, depending on the shear strain expression of specified shells. The signal equation for thin conical shell of revolution is presented next.

3. Torsion sensing of conical shells

In this section, the conventional sensing equations for conical shells are derived first, and then the fixed-free BCs and corresponding modal functions are specified. The Lamé parameters of general shells are replaced by those of the conical shell, so that the sensing signal and modal signals can be investigated.

3.1. Sensing equation for general conical shells

Fig. 3 shows the geometry of truncated conical shell of revolution. The tri-orthogonal coordinate system (x, ψ, z) locates on the shell's neutral surface, where x is the longitudinal coordinate along the meridional line, ψ the circumferential coordinate, and z the shell's normal coordinate measured from inner shell surface outward. The shell is defined from x_1 (minor end) to x_2 (major end) in the x coordinate and from $-h/2$ to $h/2$ in the z-coordinate, where h is shell thickness. β^* is semi-vertex angel of the conical shell. u_x, u_ψ and u_z are displacements in the three directions, respectively. The Lamé parameters and radii of curvature of the conical shell are defined as $A_1 = 1$, $A_2 = x\sin\beta^*$, $R_x = \infty$, $R_\psi = x\tan\beta^*$. Its cross section is also shown in Fig. 4.

Assume that the sensor is thin as compared with the conical shell structure, its elastic effect can then be neglected, and it shares the same shear strains with the shells. For thin truncated conical shell of revolution, the strains can be obtained

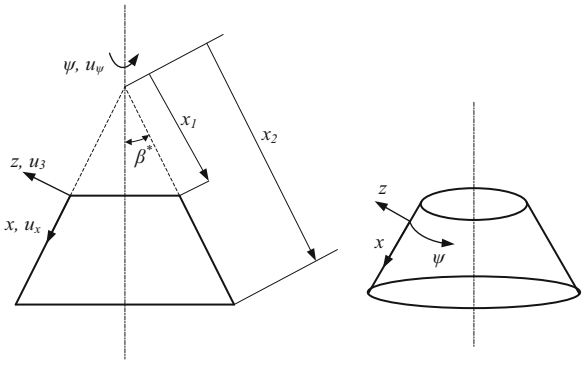

Fig. 3. Geometry of the truncated conical shell.

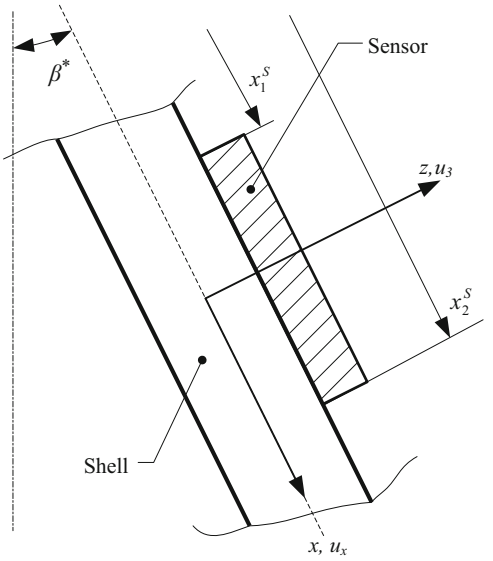

Fig. 4. Cross section of conical shells.

based on the Love's assumptions [19]

$$S_{xx} = S^0_{xx} + rk_{xx}, \tag{16a}$$

$$S_{\psi\psi} = S^0_{\psi\psi} + rk_{\psi\psi}, \tag{16b}$$

$$S_{x\psi} = S^0_{x\psi} + 2rk_{x\psi} \tag{16c}$$

where r is the distance measured from the neural surface of the conical shell taken positive in the z-coordinate. The strain items in Eq. (16) are given as

$$S^0_{xx} = \frac{\partial u_x}{\partial x}, \tag{17a}$$

$$k_{xx} = -\frac{\partial^2 u_3}{\partial x^2}, \tag{17b}$$

$$S^0_{\psi\psi} = \frac{1}{x\sin\beta^*}\frac{\partial u_\psi}{\partial \psi} + \frac{u_x}{x} + \frac{u_3}{x\tan\beta^*}, \tag{17c}$$

$$k_{\psi\psi} = -\frac{1}{x^2\sin^2\beta^*}\frac{\partial^2 u_3}{\partial \psi^2} - \frac{1}{x}\frac{\partial u_3}{\partial x}, \tag{17d}$$

$$S^0_{x\psi} = \frac{1}{x\sin\beta^*}\frac{\partial u_x}{\partial \psi} + \frac{\partial u_\psi}{\partial x} - \frac{u_\psi}{x}, \tag{17e}$$

$$k_{x\psi} = -\frac{1}{x\sin\beta^*}\frac{\partial^2 u_3}{\partial x\partial \psi} - \frac{1}{x}\frac{\partial u_3}{\partial \psi} \tag{17f}$$

For torsional vibrations, the displacements in x- and z-directions are negligible [20], thus the modal functions in the x- and z-directions are set as zero. Then, rearranging Eqs. (17) yields

$$S^0_{xx} = 0, \quad S^0_{\psi\psi} = 0, \quad k_{xx} = 0, \quad k_{\psi\psi} = 0, \quad k_{x\psi} = 0 \tag{18a–d, f}$$

$$S^0_{x\psi} = \frac{\partial u_\psi}{\partial x} - \frac{u_\psi}{x} \tag{18e}$$

Substituting them into Eqs. (16) yields the total strain

$$S_{xx} = 0, \quad S_{\psi\psi} = 0, \tag{19a, b}$$

$$S_{x\psi} = \frac{\partial u_\psi}{\partial x} - \frac{u_\psi}{x} \tag{19c}$$

Eq. (19) indicates that, in torsional vibration of conical shells, the non-nil strain $S_{x\psi}$ is a function of the circumferential modal displacement. By substituting the in-plane shear strain into the general sensing equation, one gets the sensing signal of conical shell

$$\phi = \frac{h_{15}}{S^e}\int_x\int_\psi\int_z\left(\frac{\partial u_\psi}{\partial x}-\frac{u_\psi}{x}\right)x\sin\beta^*\,dx\,d\psi\,dz \tag{20}$$

Note that the BCs are not specified in the signal derivation. Thus, Eq. (20) holds with all BCs. Eq. (20) can also be used to determine the modal participation factors. Or in the converse way, it can be used to determine the amplitudes in the modal shape functions by using an array of sensor segments or patches.

Eq. (20) gives the torsional sensing signals of shear-type piezoelectric sensors laminated on the conical shell. The signal is an averaged voltage over its electrode area. To acquire the distributed modal voltages (i.e., signal at any point of the piezoelectric patch during the free vibration of conical shell), one should decrease the electrode area of the piezoelectric patch. While the area is extremely small, the average over the electrode area can be neglected. Since the sensor's thickness is constant, the area is only a function of x, so is the shear strain. Decreasing the patch's length to zero produces the local sensing signal on the shell

$$\phi^s = \frac{h_{15}}{h^S}\int_\psi\int_z\left(\frac{\partial u_\psi}{\partial x}-\frac{u_\psi}{x}\right)x\sin\beta^*\,d\psi\,dz \tag{21}$$

Considering the axisymmetric characteristics of torsional vibrations, the sensing signals along any generating line can represent the torsion behavior of the shell as a whole. This formulation is applied to a clamped-free conical shell next.

3.2. Torsion sensor for fixed-free conical shells

It is assumed that the major end is clamped and the minor end is free. Corresponding modal functions are specified, and then the sensing expressions for conical shell with fix-free BCs are proposed in this section.

3.2.1. Mode functions

The BCs at the clamped end $x=x_2$ can be written as

$$u_x = u_\psi = u_3 = 0 \tag{22}$$

To satisfy the constrains, the displacement functions of the neutral surface are further assumed as [21]

$$u_x(x,\psi,t) = U_x(x)\cos(n\psi)\sin(\omega t) \tag{23a}$$

$$u_\psi(x,\psi,t) = U_\psi(x)\sin(n\psi)\sin(\omega t) \tag{23b}$$

$$u_3(x,\psi,t) = U_3(x)\cos(n\psi)\sin(\omega t) \tag{23c}$$

where u_x, u_ψ and u_3 are the displacements in x-, ψ- and z-directions, respectively, ω is the natural torsion frequency, t denotes the variable time, n is the circumferential wave number, $n=0, 1, 2, \ldots$, U_x, U_ψ, U_3 are functions of x

$$U_x(x) = (x-x_2)\sum_{i=0}^{I}A_i x^i \tag{24a}$$

$$U_\psi(x) = (x-x_2)\sum_{j=0}^{J}B_j x^j \tag{24b}$$

$$U_3(x) = (x-x_2)\sum_{k=0}^{K}C_k x^k \tag{24c}$$

where A_i, B_j, C_k are arbitrary coefficients, I, J, K are constants defining the order of the modal functions. These parameters can be determined by using a Ritz's procedure.

3.2.2. Sensing equation for fixed-free conical shells

Eqs. (23 and 24) are modal functions for general shell vibrations. For conical shell in torsion motion, the displacement functions in the x- and z-direction are set to be zero. As an alternative, the modal functions reduce to

$$u_\psi(x,\,\psi,\,t) = U_\psi(x)\sin(\omega t) \tag{25}$$

where $U_\psi(x)$ is defined in Eq. (24b). Substituting Eq. (25) into the in-plane shear strain Eq. (19c) yields

$$S_{x\psi} = \sum_{j=0}^{J}B_j\left[jx^j+(1-j)x_2x^{j-1}\right] \tag{26}$$

Consequently, the torsional sensing signal in Eq. (20) becomes

$$\phi^s = \frac{h^S h_{15}}{S^e} \int_x \int_\psi \sum_{j=0}^{J} B_j \left[j x^j + (1-j) x_2 x^{j-1} \right] x \sin\beta^* \, dx \, d\psi \tag{27}$$

The sensor is located from x_1^S to x_2^S in the x-direction, and from ψ_1^S to ψ_2^S in the ψ-direction. Its electrode area and sensing signal become

$$\phi^s = \frac{h^S h_{15}}{S^e} (\psi_2^S - \psi_1^S) \int_{x_1^S}^{x_2^S} \sum_{j=0}^{J} B_j \left[j x^j + (1-j) x_2 x^{j-1} \right] x \sin\beta^* \, dx \tag{28}$$

$$S^e = h^S (x_2^S - x_1^S) \tag{29}$$

The distributed torsional sensing signal resulting from the shear-type piezoelectric sensor becomes

$$\phi^s = h_{15} (\psi_2^S - \psi_1^S) x \sin\beta^* \sum_{j=0}^{J} B_j [j x^j + (1-j) x_2 x^{j-1}] \tag{30}$$

Furthermore, modal sensing characteristics of transverse shell modes with a diagonal sensor strip and a fully distributed sensor are presented next.

4. Transverse sensing of conical shells

Transversely polarized piezoelectric patches are used in sensing of transverse vibrations of conical shells. The patches are polarized in the thickness direction and the electrodes are on the top and bottom surfaces. The sensor in this arrangement is sensitive to transverse modes and insensitive to in-plane shear strains.

4.1. Sensing signals

The thin piezoelectric layer is laminated on the top surface of the conical shell. For free vibrations, the modal sensing signals are written as [9]

$$\phi^s = \frac{h^S}{S^e} \int_x \int_\psi (h_{31} S_{xx} + h_{32} S_{\psi\psi}) x \sin\beta^* \, d\psi \, dx \tag{31}$$

$$S^e = \int_x \int_\psi x \sin\beta^* \, d\psi \, dx \tag{32}$$

By substituting the displacement Eqs. (23–24) into the strain terms in Eq. (17), and removing the sine items, one gets

$$S_{xx}^0 = \cos(n\psi) \left[\sum_{i=0}^{I} (1+i) A_i x^i - x_2 \sum_{i=0}^{I} i A_i x^{i-1} \right] \tag{33a}$$

$$k_{xx} = -\cos(n\psi) \left[\sum_{k=0}^{K} (k+1) k C_k x^{k-1} - x_2 \sum_{k=0}^{K} k(k-1) C_k x^{k-2} \right] \tag{33b}$$

$$S_{\psi\psi}^0 = \frac{n\cos(n\psi)}{\sin\beta^*} (x - x_2) \sum_{j=0}^{J} B_j x^{j-1} + \cos(n\psi)(x - x_2) \sum_{i=0}^{I} A_i x^{i-1} + \frac{1}{\tan\beta^*} \cos(n\psi)(x - x_2) \sum_{k=0}^{K} C_k x^{k-1} \tag{33c}$$

$$k_{\psi\psi} = \frac{n^2 \cos(n\psi)}{\sin^2\beta^*} \left[(x - x_2) \sum_{k=0}^{K} C_k x^{k-2} \right] - \cos(n\psi) \left[\sum_{k=0}^{K} (1+k) C_k x^{k-1} - x_2 \sum_{k=0}^{K} k C_k x^{k-2} \right] \tag{33d}$$

Substituting Eqs. (32–33) into Eq. (31), one gets the total sensing voltage expression for each mode.

4.2. Signal formulations for full and diagonal sensors

If the piezoelectric layer is fully laminated on the conical shell, the interval of an integral is defined from x_1 to x_2 in the x-direction and from 0 to 2π in the ψ-direction. The sensing signal in Eqs. (31 and 32) becomes

$$\phi^s = \frac{h^S}{S^e}\int_{x_1}^{x_2}\int_{0}^{2\pi}(h_{31}S_{xx}+h_{32}S_{\psi\psi})x\sin\beta^*\,d\psi\,dx \tag{34}$$

$$S^e = \int_{x_1}^{x_2}\int_{0}^{2\pi} x\sin\beta^*\,d\psi\,dx. \tag{35}$$

In the diagonal configuration, a narrow piezoelectric stripe is diagonally laminated on the conical shell, as shown in Fig. 5. Assume the stripe is defined from x_1 to x_2 in the x-direction and 0–α in the ψ-direction; its width is w in the circumferential direction. The location of the stripe can be described by

$$\begin{cases} x_1 \le x \le x_2 \\ \dfrac{x-x_2}{x_1-x_2}\alpha-\dfrac{w}{2} \le \psi \le \dfrac{x-x_2}{x_1-x_2}\alpha+\dfrac{w}{2} \end{cases} \tag{36}$$

As a result, the total sensing signal becomes

$$\phi^s = \frac{h^S}{S^e}\int_{x_1}^{x_2}\int_{\frac{x-x_1}{x_2-x_1}\alpha-\frac{w}{2}}^{\frac{x-x_1}{x_2-x_1}\alpha+\frac{w}{2}}(h_{31}S_{xx}+h_{32}S_{\psi\psi})x\sin\beta^*\,d\psi\,dx \tag{37}$$

$$S^e = \int_{x_1}^{x_2}\int_{\frac{x-x_1}{x_2-x_1}\alpha-\frac{w}{2}}^{\frac{x-x_1}{x_2-x_1}\alpha+\frac{w}{2}} x\sin\beta^*\,d\psi\,dx. \tag{38}$$

Note that the signal expressions have the same format for both full and diagonal sensors, except for the interval of integral defining the sensor shape or region. Eqs. (37–38) are applicable for general diagonal sensing. For example, by setting α=0, the sensor stripe responds to the longitudinal direction, as shown in Fig. 6a. The influence of the circumferential deformation in the ψ-direction on the sensing signal is negligible. Or, by setting $\alpha\to\infty$, the stripe is sensitive to circumferential deformations and vibrations along circumferential direction, as shown in Fig. 6b. Here, the longitudinal influence of the signal generation is also negligible.

4.3. Distributed sensing signals

The sensing Eq. (31) represents the sensing signal of a piezoelectric stripe laminated on the conical shell. It is an averaged voltage over the sensor area. Reducing the sensor area to infinitesimally small, the area average can be neglected and signal becomes the point sensing voltage at any point of the sensor patch. The global distributions of these signals reveal the mode shape of the conical shell, i.e., the modal signals. The sensing signal now becomes [9]

$$\phi^s(x,\psi) = h^s(h_{31}S_{xx}+h_{32}S_{\psi\psi}) \tag{39}$$

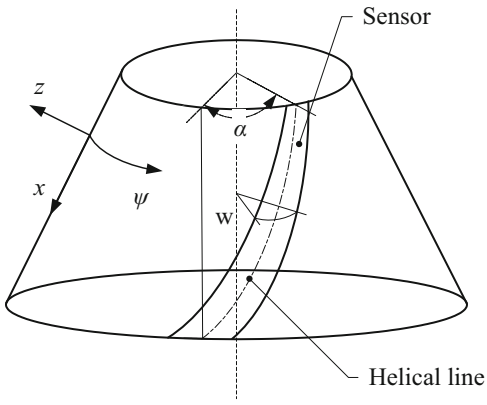

Fig. 5. Diagonal sensor stripe.

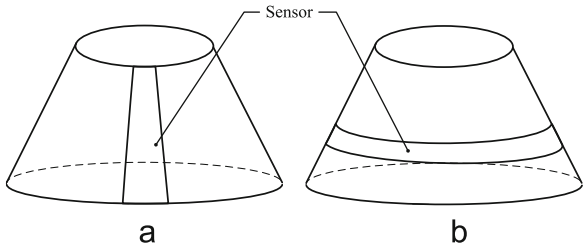

Fig. 6. Alternatives of general diagonal sensor: (a) longitudinal sensor, $\alpha=0^\circ$ and (b) circumferential sensor, $\alpha\to\infty$.

Substituting Eqs. (16) into the signal equation yields

$$\phi^s(x,\psi)=h^s h_{31}S^0_{xx}+h_{31}r^s k_{xx}+h^s h_{32}S^0_{\psi\psi}+h^s h_{32}r^s k_{\psi\psi} \tag{40}$$

The modal signal consists of four components related to the four strains, i.e., longitudinal membrane strain, the circumferential membrane strain, the longitudinal bending strain and the circumferential bending strain. Substituting strains into Eqs. (33) and dividing the signal into four components, one gets the individual signal generation resulting from these strain components

Component 1: signal related to longitudinal membrane strain

$$\begin{aligned}\phi^s_1(x,\psi)&=h^s h_{31}S^0_{xx}\\&=h^s h_{31}\cos(n\psi)\left[\sum_{i=0}^{I}(1+i)A_i x^i-x_2\sum_{i=0}^{I}iA_i x^{i-1}\right]\end{aligned} \tag{41a}$$

Component 2: signal related to longitudinal bending strain

$$\begin{aligned}\phi^s_2(x,\psi)&=h^s h_{31}r^s_x k_{xx}\\&=-h^s h_{31}r^s_x\cos(n\psi)\left[\sum_{k=0}^{K}(k+1)kC_k x^{k-1}-x_2\sum_{k=0}^{K}k(k-1)C_k x^{k-2}\right]\end{aligned} \tag{41b}$$

Component 3: signal related to circumferential membrane strain

$$\begin{aligned}\phi^s_3(x,\psi)&=h^s h_{31}S^0_{\psi\psi}\\&=h^s h_{32}\left[\frac{n\cos(n\psi)}{\sin\beta^*}(x-x_2)\sum_{j=0}^{J}B_j x^{j-1}+\cos(n\psi)(x-x_2)\sum_{i=0}^{I}A_i x^{i-1}+\frac{1}{\tan\beta^*}\cos(n\psi)(x-x_2)\sum_{k=0}^{K}C_k x^{k-1}\right]\end{aligned} \tag{41c}$$

Component 4: signal related to circumferential bending strain

$$\begin{aligned}\phi^s_4(x,\psi)&=h^s h_{32}r^s_\psi k_{\psi\psi}\\&=h^s h_{32}r^s_\psi\left\{\frac{n^2\cos(n\psi)}{\sin^2\beta^*}\left[(x-x_2)\sum_{k=0}^{K}C_k x^{k-2}\right]-\cos(n\psi)\left[\sum_{k=0}^{K}(1+k)C_k x^{k-1}-x_2\sum_{k=0}^{K}kC_k x^{k-2}\right]\right\}\end{aligned} \tag{41d}$$

The modal signals and their contributing components are evaluated in the following case studies.

5. Case studies

Consider an isotropic truncated conical shell model with its major end clamped and the minor end free. Geometric parameters of the shell are listed in Table 1. The parameters in the modal functions I, J, K are chosen as $I=J=K=2$, the coefficients items A_i, B_j, C_k are solved by using the Ritz method. The modal functions are used as the modal displacements for each shell modal. The amount of each modal participation in the dynamic response is assumed to be 1. The piezoelectric parameters h_{31}, h_{32} and h_{15} are assumed to be 1 too. Therefore, if multiply the sensing signals with the practical piezoelectric parameters and the modal participation factors, the dynamic sensing signals of forced vibrations of the conical shell can be attained with unit in volt.

5.1. Distributed signals of torsional vibrations

Recall that the signal generation of axisymmetric torsional vibrations of the conical shell with the shear-type piezoelectric sensor was defined previously. The sensing signals along any meridional line represent the torsional behavior of the shell as a whole. Figs. 7 and 8 show the distributed sensing signals of torsional modes of the conical shell. The sensing signal of first mode increases with x, and get the maximum value nearby the major end, then the amplitude decreases, as shown in Fig. 7. For signal of the second mode, the sensing signal first increases and then decreases with

Table 1
Parameters of the model.

Item	Value	Unit
x_1	0.2	m
x_2	0.5	m
β^*	$\pi/4$	rad
h	0.005	m
w	0.174	rad
r^S	0.0025	m
α	$\pi/4$	rad
h_{31}	1	V/m
h_{32}	1	V/m
h_{15}	1	V/m

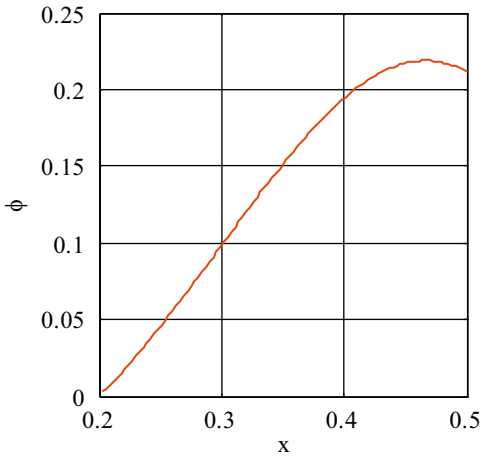

Fig. 7. Modal voltage for the first torsional mode of truncated conical shell.

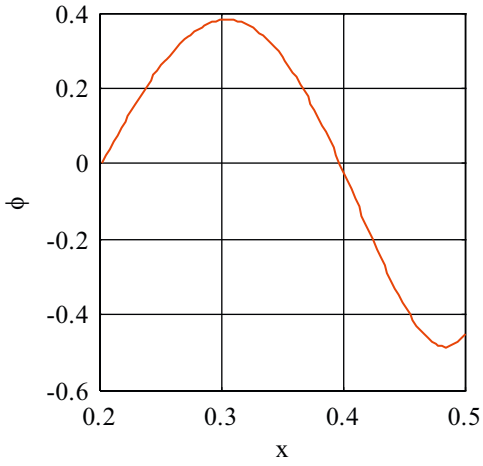

Fig. 8. Modal voltage for the second torsional mode.

respect to x, as shown in Fig. 8. Two peaks appear, the first at x=0.31 m and the other at x=0.48 m. At the location of x=0 and 0.4 m, the sensing signals are zero. Both curves are identical to the modal shapes.

The sensing signals indicate that, to sense the first torsional mode, the optimal location for the shear-type piezoelectric sensor is at x=0.46 m. For the second torsional mode, the optimal locations are x=0.48 and 0.31 m. If two sensors are employed, one is at the x=0.31 m and the other at x=0.48 m, then the phase difference between the two signals is 180°. On the other hand, if mode 1 is the desired mode and mode 2 to be avoided, the optimal location for the sensor is at x=0.40 m.

5.2. Distributed signals of transverse vibrations.

Both full and diagonal sensing of two mode groups ($n=1, 2$) of the truncated conical shell are evaluated. In each mode, the four signal components are calculated and plotted. There are six component plots in each modal signal generation group.

The top-left plot shows distributed sensing signals induced by the longitudinal membrane strain; the top-right shows signals induced by the longitudinal bending strain; the middle-left and middle-right plots are signals induced by the circumferential membrane strain and the circumferential bending strain, respectively; the bottom-left shows the overall distributed sensing signal; and the bottom-right shows the mode shape of each mode. Curve surfaces denote the distributed amplitudes of sensing signals; the translucence plane (4×4 dot line grids) denotes the zero amplitude of sensing voltage, used as a reference. The red stripe denotes sensing signals of the diagonal piezoelectric sensor.

5.2.1. n=1 Mode group

The first two modal signals and their components of $n=1$ mode group are plotted in Figs. 9 and 10. In this mode group, the total signals are mainly contributed by the component $\phi_3^s(x, \psi)$ related to the circumferential membrane strain. The signals at the minor end are lower. The signals at the major are mainly contributed by the component $\phi_2^s(x,\psi)$ related to the longitudinal bending strain. The distribution of signals indicates the strain amplitudes as well as the phase of the shell strain.

In the (1, 1) mode, the dominant component of the total signals is $\phi_2^s(x,\psi)$ related to the longitudinal bending strain, as shown in Fig. 9. The total signals attain the maximum value at the region nearby the major end, and become lower at the

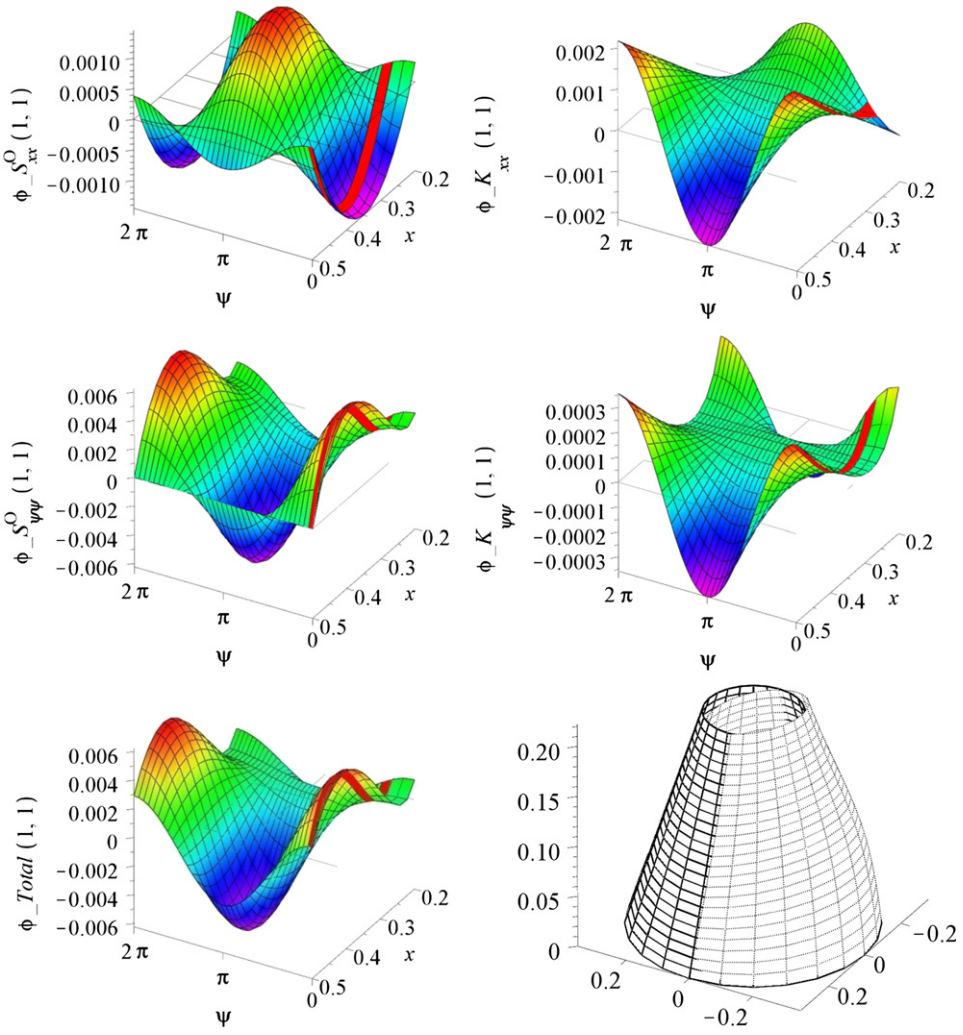

Fig. 9. Sensing signals of mode (1, 1).

ends. The signal components related to the membrane strain attain the maximum at the region nearby the major end, and the other two components related to the bending strain attain the maximum values at the ends.

The sending signals of mode (1, 2) are shown in Fig. 10. The signal $\phi_3^s(x, \psi)$ becomes the dominant component of the total signals, just as that in mode (1, 1). The other signal components get the maximum values at the minor end, but the signals of $\phi_1^s(x, \psi)$ and $\phi_2^s(x, \psi)$ have a phase difference of 180°. As a result, the total signals at that end are much lower. At the major end, the total signals are mainly contributed by the $\phi_2^s(x, \psi)$.

5.2.2. n=2 Mode group

The modal signals and the four components of $n=2$ mode group are investigated and plotted in Figs. 11 and 12. Based on the distribution of total signals and the components, the optimal locations of piezoelectric sensors for sensing the desired mode or strain components can be found.

In mode (2, 1), the total signals are mainly contributed by the components $\phi_3^s(x, \psi)$ and $\phi_4^s(x, \psi)$, as shown in Fig. 11. The maximum values of the total signals are acquired at the region near the minor end. The signal amplitudes of components $\phi_1^s(x, \psi)$ and $\phi_2^s(x, \psi)$ are higher at the major end, but they have opposite phase. Therefore, the total signals at the end are much lower. The results indicate that, at the major end, the strain items S_{xx}^0 and k_{xx} are higher, and nearby the minor end, the strain $S_{\psi\psi}^0$ and $k_{\psi\psi}$ become dominant.

Fig. 12 shows the signals of mode (2, 2). The total signals show similar trends with the $\phi_3^s(x, \psi)$ components. At the region nearby the major end, the total signals are mainly contributed by the components $\phi_1^s(x, \psi)$ and $\phi_2^s(x, \psi)$, and at the other end, the component $\phi_3^s(x, \psi)$ becomes dominant.

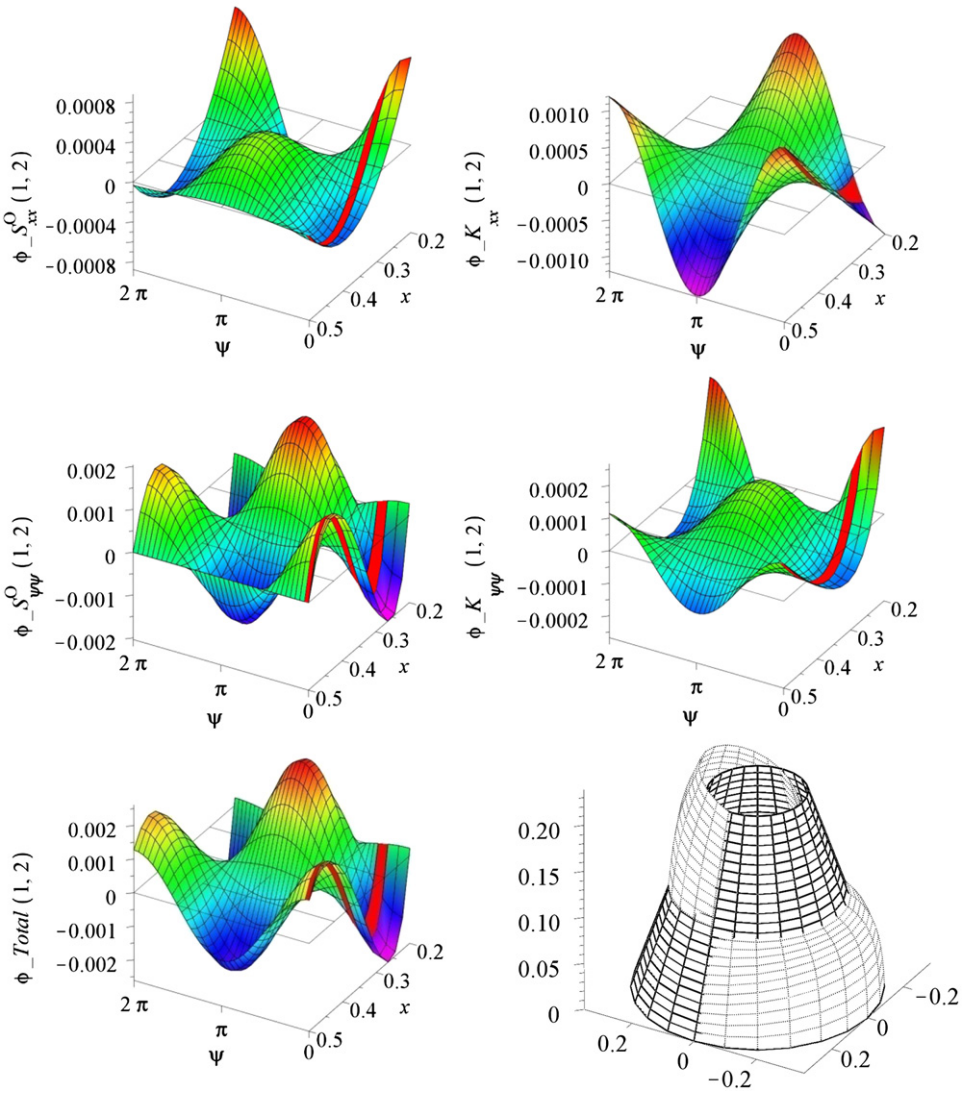

Fig. 10. Sensing signals of (2, 1) mode.

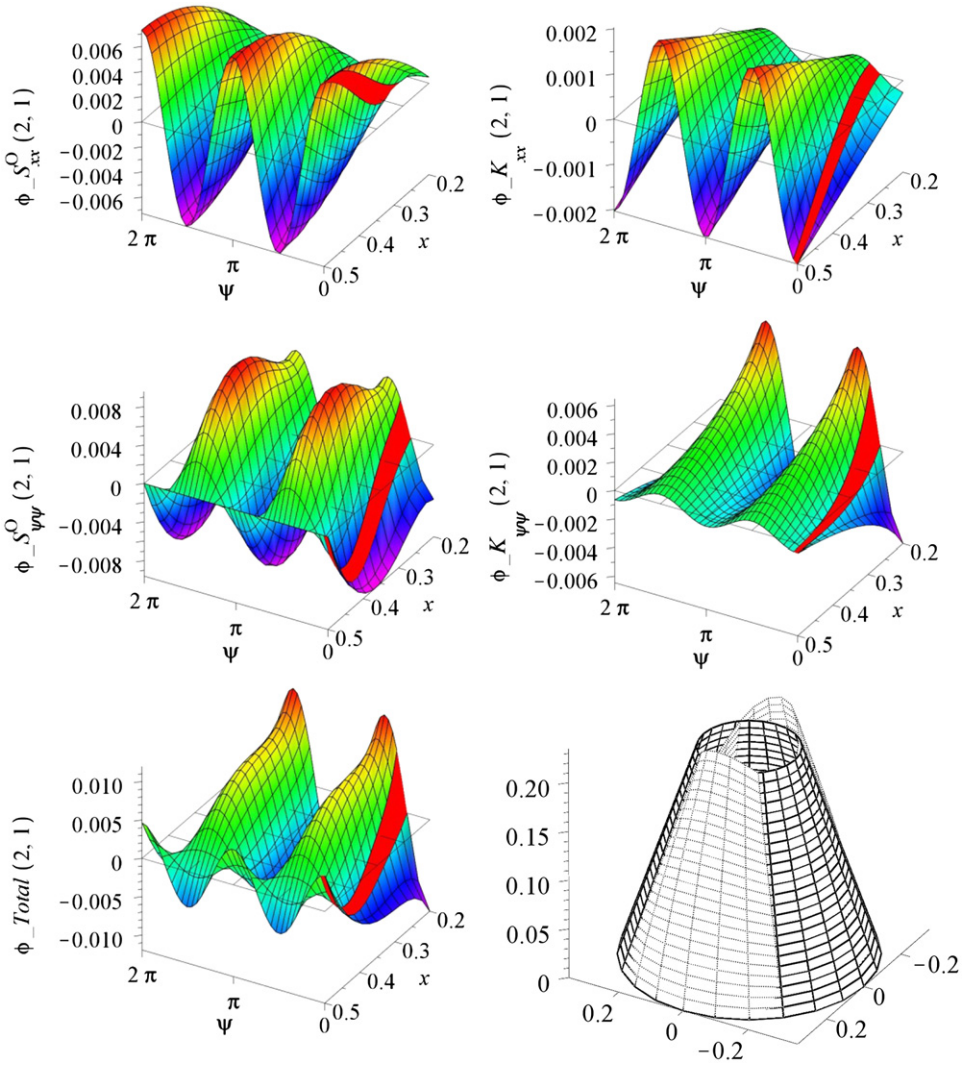

Fig. 11. Sensing signals of (1, 2) mode.

The numerical results indicate the optimal locations of each mode for the sensors. If one mode is desired, the sensor can be located at the region with maximum amplitude of the signals. Generally, several sensors are needed to sense the vibration of shells. Assuming that the sensors located at the region above the zero plane in Figs. 9–12 output positive signals, then the sensors under the zero plane will output negative signals at the same time. Or on the other hand, the sensor can be located at the region with zero signals to avoid this mode.

6. Conclusions

A diagonal piezoelectric sensor was proposed. The sensing signal equations of shear- and biaxial-type piezoelectric sensors were derived. The BCs of the truncated conical shell were clamped at the major end and free at the minor end.

An analytical procedure was presented for estimating sensing signals of generic shells of revolution in torsion using shear-type piezoelectric sensors. It was simplified to conical shells of revolution. Then, sensing equations and modal signals for clamped-free conical shells were derived. To study the free transverse vibration, distributed sensing signals and four contributing components were investigated in detail.

The modal signals and the components of a clamped-free conical shell modal were evaluated. Three mode groups were calculated, including the torsional, lateral and transverse vibrations; and the resultant signal distributions were plotted. The results show the sensing signals are higher at regions with higher shear strains. In low order free modes, the mode shape is similar to the distribution of the circumferential membrane signal, i.e., $S^0_{\psi\psi}$, which dominates the total signal generations. In the first two modes of both $n=1$ and $n=2$ modes, the two bending signals show almost the same amplitudes and spatial distributions. The regions with high modal signal amplitudes are the optimal locations for the sensor

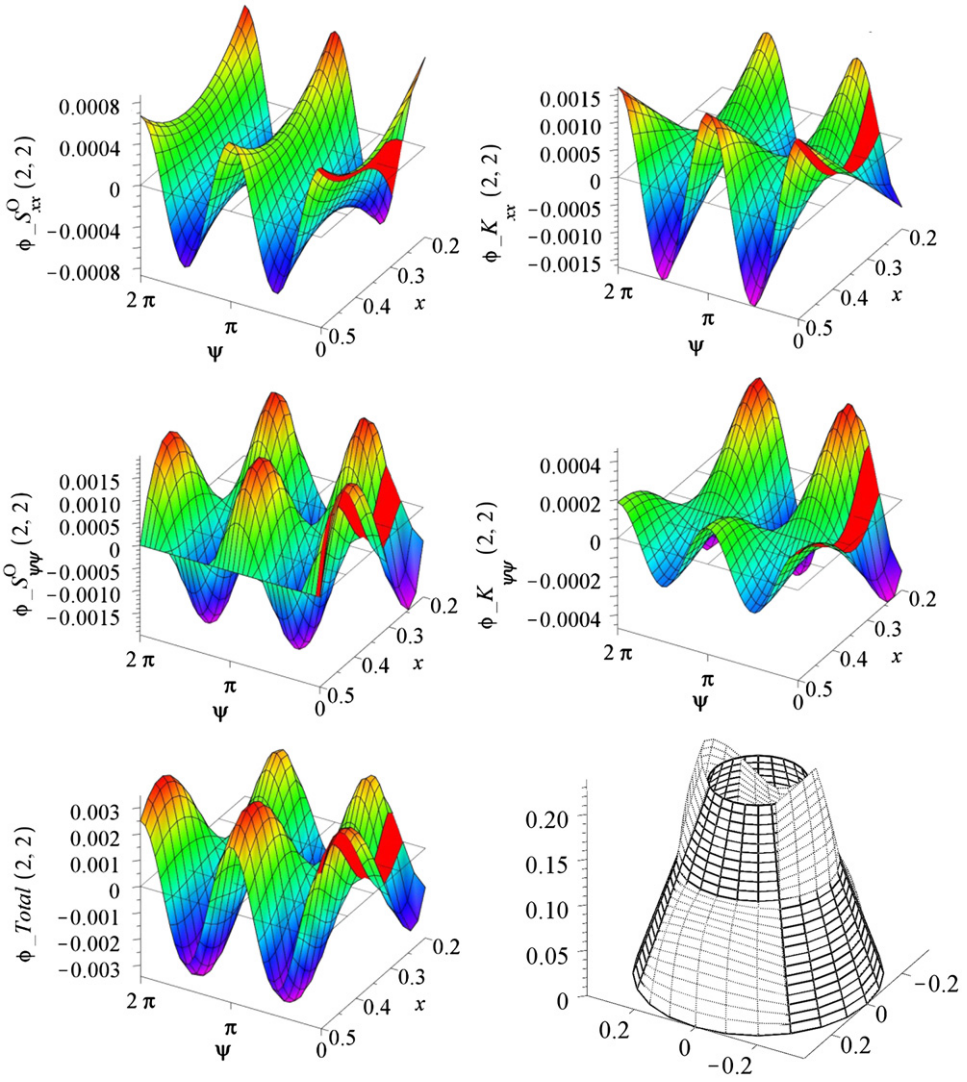

Fig. 12. Sensing signals of (2, 2) mode.

placements to monitor these natural modes. Also, this method is applicable for determining the modal participation factors, or by using several sensors, it is capable of determining the mode shapes.

Acknowledgments

This research is supported by "Beforehand Research Project of Civil Space" (C4120062301) at COSTIND and "111 Project" (B07018) at the Harbin Institute of Technology.

References

[1] J. Zhang, Y. Chen, J. Luo, H.-X. Hua, Review of the whole-spacecraft isolation techniques, Hangkong Xuebao/Acta Aeronautica et Astronautica Sinica 26 (2005) 179–183.
[2] J.R. Maly, S.A. Haskett, P.S. Wilke, E.C. Fowler, D. Sciulli, T.E. Meink, ESPA: EELV Secondary Payload Adapter with whole-spacecraft isolation for primary and secondary payloads, Smart Structures and Materials 2000: Damping and Isolation, Newport Beach, CA, USA, 2000.
[3] D. Thakkar, R. Ganguli, Induced shear actuation of helicopter rotor blade for active twist control, Thin-Walled Structures 45 (2007) 111–121.
[4] A.K. Jha, D.J. Inman, Piezoelectric actuator and sensor models for an inflated toroidal shell, Mechanical Systems and Signal Processing 16 (2002) 97–122.
[5] H.S Tzou, in: Piezoelectric shell—Distributed Sensing and Control of Continua, Kluwer Academic Publishers, Boston/Dordrecht, 1993.
[6] N. Wakatsuki, Y. Kagawa, M. Haba, Tri-axial sensors and actuators made of a single piezoelectric cylindrical shell, IEEE Sensors Journal 4 (2004) 102–107.

[7] X.H. Wu, C.Q. Chen, Y.P. Shen, X.G. Tian, A high order theory for functionally graded piezoelectric shells, International Journal of Solids and Structures 39 (2002) 5325–5344.
[8] J. Callahan, H. Baruh, Modal sensing of circular cylindrical shells using segmented piezoelectric elements, Smart Materials & Structures 8 (1999) 125–135.
[9] H.S. Tzou, W.K. Chai, D.W. Wang, Modal voltages and micro-signal analysis of conical shells of revolution, Journal of Sound and Vibration 260 (2003) 589–609.
[10] C.-T. Sun, X.R. Zhang, Use of thickness-shear mode in constructing adaptive sandwich structures, Smart Structures and Materials 1995: Smart Structures and Integrated Systems, San Diego, CA, USA, 1995.
[11] A.E. Glazounov, Q.M. Zhang, C. Kim, Torsional actuator based on mechanically amplified shear piezoelectric response, Sensors and Actuators A: Physical 79 (2000) 22–30.
[12] A. Benjeddou, J.F. De, Piezoelectric transverse shear actuation and sensing of plates, Part 1: A three-dimensional mixed state space formulation, Journal of Intelligent Material Systems and Structures 12 (2001) 435–449.
[13] B.P. Baillargeon, S.S. Vel, Active vibration suppression of sandwich beams using piezoelectric shear actuators: experiments and numerical simulations, Journal of Intelligent Material Systems and Structures 16 (2005) 517–530.
[14] L.K. Liu, L. Liang, G.T. Zheng, W.H. Huang, Dynamic design of octostrut platform for launch stage whole-spacecraft vibration isolation, Journal of Spacecraft and Rockets 42 (2005) 654–662.
[15] J.R. Jarosh, G.S. Agnes, G.G. Karahalis, Adaptive control for payload launch vibration isolation, smart structures and materials, Damping and Isolation 4331 (2001) (2001) 162–174.
[16] C.-C. Sung, V.V. Varadan, X.-Q. Bao, V.K. Varadan, Active control of torsional vibration using piezoceramic sensors and actuators, 31st AIAA/ASME/ASCE/AHS/ASC Structures, Structural Dynamics and Materials Conference, Long Beach, CA, USA, 1990.
[17] G.D. Luan, J.Z. Zhang, R.Q Wang, in: Piezoelectric Transducers and Arrays, Peking University Press, BeiJing, 2005.
[18] J.S. Yang, H.Y. Fang, Q. Jiang, A vibrating piezoelectric ceramic shell as a rotation sensor, Smart Materials & Structures 9 (2000) 445–451.
[19] Z.L. Xu (Ed.), Elasticity, fourth ed., vol. 2, Higher Education Press, Beijing, 2006.
[20] W. Soedel, Vibrations of shells and plates, Mechanical Engineering, third ed., Marcel Dekker Inc., New York, 2004.
[21] A.W. Leissa, J.-H. Kang, Three-dimensional vibration analysis of thick shells of revolution, Journal of Engineering Mechanics 125 (1999) 1365–1371.